Potential faster Arctic sea ice retreat triggered by snowflakes' greenhouse effect

Jui-Lin Frank Li[1], Mark Richardson[1,2], Wei-Liang Lee[4], Eric Fetzer[1], Graeme Stephens[1], Jonathan Jiang[1] Yulan Hong[3], Yi-Hui Wang[6], Jia-Yuh Yu[7], Yinghui Liu[5]

5   [1]Jet Propulsion Laboratory, California Institute of Technology, Pasadena, CA 91125, USA
[2]Joint Institute for Regional Earth System Science and Engineering, University of California, Los Angeles, CA 90095-7228 USA
[3]Department of Earth, Ocean and Atmospheric Science, Florida State University, Tallahassee, FL 32304, USA
10   [4]RCEC, Academia Sinica, Taiwan
[5]Cooperative Institute for Meteorological Satellite Studies, University of Wisconsin, Madison, WI 53706, USA
[6]Center for Coastal Marine Sciences, California Polytechnic State University, San Luis Obispo, CA 93407, USA
15   [7]Department of Atmospheric Sciences, National Central University, Taoyuan City, 32001, Taiwan

Correspondence to: J-L Frank Li (Juilin.F.Li@jpl.nasa.gov)

Abstract. Recent Arctic sea ice retreat has been quicker than in most general circulation model (GCM) simulations. Natural factors may have amplified this, but reliable attribution and projection requires accurate representation of relevant physics. Most current GCMs don't fully represent falling ice radiative
20   effects (FIRE), and here we show that the small set of Coupled Model Intercomparison Project, phase 5 (CMIP5) models that include FIRE tend to show faster observed retreat. We investigate this using controlled simulations with the CESM1-CAM5 model. Under 1pctCO2 simulations, including FIRE results in the first occurrence of an "ice free" Arctic (extent $< 1{\times}10^6$ km^2) at 550 ppm CO_2, compared with 680 ppm otherwise. Over 60—90 °N oceans, snowflakes reduce downward shortwave and increase
25   downward longwave, improving agreement with the satellite-based CERES-EBAF surface dataset. We propose that snowflakes' equivalent greenhouse effect results in fewer safe spaces in which sea ice can thicken during winter, resulting in a thinner pack whose retreat is more easily triggered by global warming. This is supported by the controlled CESM1-CAM5 simulations, but this explanation does not apply across the CMIP5 ensemble where other processes can dominate. Regardless, we show that FIRE

can substantially change Arctic sea ice projections and propose that better including falling ice radiative effects in models is a high priority.

1 Introduction

The Arctic region is undergoing pronounced change, becoming warmer and wetter (Boisvert and Stroeve, 2015) while its land ice melts (Jacob et al., 2012; Kjeldsen et al., 2015) and spring arrives weeks earlier than in the 1990s (Post et al., 2018). Communities in the region may have to adapt to changing hunting seasons (Rolph et al., 2018), loss of coast that was previously protected by sea ice (Overeem et al., 2011) and the surface destabilisation due to permafrost melt (Shiklomanov et al., 2017).

In particular, Arctic sea ice retreat potentially opens area for resource extraction or transport routes (Smith and Stephenson, 2013) and has national security implications for neighbouring states. Physically, ice affects both top-of-atmosphere and surface heat fluxes. In winter it insulates the ocean, restricting the leakage of heat to space via infrared cooling, and in summer it predominantly reflects sunlight and cools the surface (Tietsche et al., 2011). From a surface perspective, it restricts evaporation and therefore affects the hydrological cycle (Bintanja and Selten, 2014). It has been proposed that reduced sea-ice extent may further smooth the latitudinal temperature gradient, thus weakening the high latitude jets and making it easier to shift into a "wavy" pattern, which is associated with long-lived extreme events at mid latitudes (Francis and Vavrus, 2012). However, these proposed impacts at lower latitudes are currently speculative and disputed (Cohen et al., 2014).

The recent rapid Arctic sea ice retreat included extreme minima in 2007 and 2012 which received particular attention. Regarding the 2007 minimum, a reduction in cloudiness during the melt season relative to previous years was shown to change surface energy balance by enough to thin sea ice by up to 0.3 m over three months (Kay et al., 2008).

Natural atmospheric & ocean dynamics may also contribute by exporting ice to lower latitudes, which tends to increase extent in winter but ultimately reduce it in summer. For example, surface pressure observations have been used to infer contributions due to anomalously high ice export through the Pacific sector in 2007 (Zhang et al., 2008) and the Fram Strait in 2012 (Smedsrud et al., 2017).

From analyses of subsets of climate models in the Climate Model Intercomparison Project, phase 5 (CMIP5 (Taylor et al., 2012)), the observed extreme low events and general retreating trend have been attributed to a combination of melt driven by global warming along with a likely natural component (Kay et al., 2011). One recent study suggested an equally important role for anthropogenic warming and natural

5 variability for the extreme 2012 loss (Kirchmeier-Young et al., 2017).

Reliable attribution requires the ability to quantify physical processes and relevant responses to each forcing. Accurate future projections are also necessary for informed decisions with the changing Arctic, such as by investors or insurance companies who may wish to assess the risk associated with proposals for future shipping routes. A common criterion is determining if and when a seasonally "ice free" Arctic

10 will occur, arbitrarily defined as when sea ice extent falls below 1×10^6 km^2. At this point the remaining ice would cluster around islands and coasts, leaving the basin largely open.

Climate models are crucial tools to inform projections but their Arctic response varies widely (Massonnet et al., 2012; Stroeve et al., 2012). The time at which the Arctic is likely to become "ice free" under high emissions in CMIP5, for example, ranged from 2041—2060 in Massonet et al. (2012) while Stroeve et

15 al. (2012) only stated that "a seasonally ice-free Arctic Ocean within the next few decades is a distinct possibility".

Summer retreat has been faster than the average CMIP5 model simulation, implying a large naturally forced component to recent extremes. However, if the CMIP5 models do not adequately include factors that influence the forced response then their projections will be biased. We have previously shown that

20 the majority of CMIP5 models do not properly account for atmospheric ice in their radiation codes. While they include suspended ice, falling ice is excluded and this causes region-dependent biases in the surface energy budget that, for example, tends to result in a larger mean Antarctic sea ice extent (Li et al., 2017). Here we focus on sea ice extent changes and the surface energy budget over oceans from 60—90 °N. In the simplest terms, falling ice should produce a year round increase in downward longwave radiation and

25 a decrease in surface shortwave which will be greatest in local summer. Li et al. (2017) showed that in the Antarctic this results in a dampened annual cycle with the increased wintertime longwave restricting maximum sea ice extent, which then results in a lower albedo when the sun rises again. This lower albedo counteracts somewhat the reduction in sunlight arriving at the surface due to reflection by snowflakes.

With regards to the Arctic, we expect a somewhat different expression due to (1) wintertime maximum extent being restricted by continental boundaries and boundaries with warm ocean currents, (2) generally thicker sea ice (Kurtz and Markus, 2012; Kwok and Cunningham, 2008) and (3) faster local warming under the early part of CO_2-driven heating.

5   It is therefore possible that increased winter longwave from FIRE may not have a substantial effect on sea ice extent, but may restrict its thickness. This should manifest later as a faster retreat, both during a typical summer melt season and during long-term warming. However, if the maximum extent is not strongly affected then the albedo will begin the melt season at a similar level regardless of FIRE, and therefore there will be no offset for the stronger expected downward shortwave. This will mean that a

10   non-FIRE simulation should experience more local albedo feedback due to its stronger incident sunlight. These effects should oppose each other and it is not necessarily obvious whether one factor should dominate.

As well as changes in the mean state which could affect retreat through the initial pack's robustness, it is also possible that local fluxes could vary in different ways under warming. For example, in a simulation

15   where FIRE is included, warming could raise the melting layer during summer, leading to a reduction in the total ice water path (TIWP) in favour of liquid water, which has a smaller radiative effect. The direct effect of this would be to reduce the trend in downward longwave and increase the trend in downward shortwave, relative to a simulation where FIRE is excluded. This ignores further coupling to atmospheric conditions that could similarly affect feedbacks.

20   Here we investigate the importance of FIRE using both standard CMIP5 output along with controlled simulations with a CMIP5 era climate model, the National Center for Atmospheric Research-Department of Energy (NCAR-DOE) Coupled Earth System Model version 1 with the Coupled Atmosphere Model version 5 (CESM1-CAM5). We ignore coupled dynamic responses in favour of studying the direct surface radiative flux terms to simplify the analysis.

25   The paper is structured as follows: Section 2 lists the data and methodology, Section 3 reports on the simulated & observed sea ice changes, Section 4 looks at the simulated & observed surface radiative fluxes, Section 5 synthesises and discusses the results and their limitations, and Section 6 concludes.

2 Methods and Data

2.1 CMIP5 and CESM1-CAM5 Simulations

We use outputs from the CMIP5 archive (Taylor et al., 2012) and select models who have all surface energy balance terms plus the fields necessary to calculate sea ice extent for each of the preindustrial

5 control (piControl), historical and Representative Concentration Pathway 8.5 (RCP8.5 (Riahi et al., 2011)) scenarios. The historical scenarios run through 2005, after which we append the RCP8.5 output. This is a scenario of very high radiative forcing which we select to better identify forced response over internal variability, and we make no judgment about the probability that this forcing will occur. For each model we select the first simulation in each case, r1i1p1 in CMIP5 nomenclature, which results in 25

10 simulations.

We split these into two sub-ensembles depending on whether FIRE is allowed: those including snow radiative effects (CMIP5-SoN, N = 7) and those in which there are no snow radiative effects (CMIP5-NoS, N = 18). These are listed in Supplementary Table 1.

For CESM1-CAM5 we use previously published historical simulations (Li et al., 2014), which are run on

15 a spatial resolution close to $1 \times 1°$ latitude-longitude grid. CAM5 is one of the few atmospheric models that allows snow radiative interactions, and it does this thanks to a two-moment cloud scheme with diagnostic snow (Gettelman et al., 2010; Morrison and Gettelman, 2008). This only represents the stratiform component of falling ice and not that in convective towers, but the majority of Arctic snowfall will be included. This scheme allows snow radiative effects to be allowed (CESM1-SoN) or disallowed

20 (CESM1-NoS). Unfortunately, output is not available for any RCP, which forces observational comparisons to end in 2005. To estimate the first response, we use the 1pctCO2 output, which is a simulation in which atmospheric CO_2 increases at 1 % yr^{-1} for 140 years. Radiative forcing definitions differ, but typical values for quadrupled CO_2 are 5.3—8.6 W m^{-2} (Forster et al., 2013) , meaning that total forcing is similar to the historical-RCP8.5 series used for CMIP5. We use output for fully coupled

25 CESM1-SoN and for CESM1-NoS runs following the historical and 1pctCO2 simulations.

2.2 Sea Ice Extent

Sea ice extent (SIE) is defined as the area of ocean with sea ice concentration (sic) greater than 15 %. This was originally developed for satellite-based passive microwave products to be a robust identifier of ice edges when compared against aircraft observations (Cavalieri et al., 1991). This aids with robustness

5   of the retrieval to changing weather conditions or melt ponds on the ice which may interfere with the observed brightness temperatures. For observations we use the National Snow and Ice Data Center (NSIDC) monthly series of total sea ice extent (Fetterer et al., 2017) which is calculated from gridded data on a nominal 25 km grid. We use the complete years that were available as of analysis time: 1979—2017.

10   The standard CMIP5 output is the sea ice concentration within an ocean grid cell, and we calculate sea ice extent following a previously published method (Kirchmeier-Young et al., 2017), by reporting the total area of all model grid cells with sic > 15 % (see Supplementary Figure 1 for verification of this calculation). This is not a fully consistent comparison due to differences in grid cell sizes and as observations may underestimate sea ice concentration in the presence of substantial melt ponds. Here we

15   assume that these factors have little effect on the large-scale changes under study.

2.3 Surface Energy Budget

We use $1 \times 1°$ monthly estimates of surface fluxes from the Clouds and the Earth's Radiant Energy System Energy Balanced and Filled-Surface (CERES-EBAF Surface, (Kato et al., 2013)) product, for which we have complete years for 2001—2015. This combines satellite data with a radiative transfer model to

20   estimate surface fluxes and is estimated to have a monthly root mean square error of ± 11 W m^{-2} in each term over oceans (Kato et al., 2012).

CESM1-CAM5 output is provided monthly at $1° \times 1°$ and for all CMIP5 models, we use previously gridded $2.5° \times 2.5°$ monthly data. Fluxes are calculated by taking the area-weighted average of values in each grid cell after scaling by the ocean fraction. For CERES and CESM1-CAM5 we use the CESM1-CAM5 grid,

25   and for all CMIP5 models we use a consistent map built from the $0.125° \times 0.125°$ European Center for Medium Range Weather Forecasts European Reanalysis-Interim (ECMWF ERA-Interim) land mask. For comparison of the mean state fluxes between CERES and our controlled CESM1-CAM5 simulations we

only have 4 complete years of overlap, 2001—2005. We therefore show the results for these 4 years with error bars estimated by slicing both CERES and CESM1-CAM5 post-1979 data into non-overlapping 4-year periods and taking the standard deviation of these samples. For differences these standard deviations are added in quadrature and reported as an estimate of the uncertainty. This estimate only represents the

5 effect of internal variability due to our use of a short time period.

3 Observed and Simulated Sea Ice Extent Results

Figure 1 shows the March and September post-1979 changes in SIE in NSIDC observations and CMIP5 simulations. These are the months of maximum and minimum SIE (all months are shown in Supplementary Figure 2). The upper right panel shows that observed September retreat approaches the

10 lower 10th percentile of the CMIP5 ensemble. When plotted using anomalies, the retreat falls outside the model range (Supplementary Figures 3—4).

The bottom panels of this figure show that the CMIP5-SoN sub ensemble generally agrees better with the faster observed retreat. In March, trends are similar but CMIP5-SoN shows greater extent, which is the opposite of expectations if wintertime longwave from FIRE were the main cause of differences. However,

15 differences in parameterisations for clouds, the atmosphere, oceans and sea ice can change the mean state, so to isolate FIRE we present the controlled CESM1 simulations in Figure 2.

CESM1-CAM5 captures the mean extent well with a smaller discrepancy versus observations throughout the year when including FIRE (full annual cycles in Supplementary Figures 5—6). Historical retreat is also faster in CESM1-SoN than in CESM1-NoS, but only significantly so if white noise is assumed ($t =$

20 2.39, $p = 0.012$), whereas after accounting for lag-1 autocorrelation above 0.4 the difference is insignificant ($t = 1.51$, $p = 0.073$). Neither show significant differences relative to NSIDC observations over 1979—2005 although the 1979—2017 trend is detectably faster than the CESM1-NoS changes through 2005. The bottom panels show that inclusion of FIRE results in a much faster September retreat beginning around year 40 of the simulation in the 1pctCO2 simulation.

25 To allow easier interpretation, we take overlapping decadal averages of mean SIE and the number of years within that decade with SIE $< 1 \times 10^6$ km^2, and plot these as a function of atmospheric CO_2 concentration (assuming year 0 = 280 ppm) in Figure 3. Below 2017 atmospheric CO_2 concentration, there are only

small differences in decadal mean SIE, but for concentrations higher than this the Arctic sea ice retreats far more rapidly under global warming when FIRE is included. In the CESM1-SoN simulation, the majority of years are classified as ice free once atmospheric CO_2 passes 550 ppm, compared with 680 ppm in the CESM1-NoS simulation. In a naïve sense this implies a difference of almost 100 % in

5   cumulative future anthropogenic CO_2 emissions before the Arctic commonly becomes ice free if these CESM1-CAM5 1pctCO2 simulations are representative of the real world. Figure 3 shows that the potential magnitude of FIRE on Arctic sea ice retreat is large, but we do not argue that this necessarily means a more rapid collapse of Arctic sea ice in reality. Firstly, CESM1-CAM5 may have compensating biases due to other processes and secondly the disappearance of ice under transient CO_2-driven warming

10   may not correspond to reality where a mixture of radiative forcing agents is changing. Some of these, such as aerosols, may drive stronger seasonal, regional, and dynamic responses than well-mixed greenhouse gases like CO_2 (Hansen et al., 1997).

These simulations show that falling ice radiative effects could lead to much greater Arctic sea ice retreat when the system is forced under global warming and support the inclusion of FIRE in future models.

15   Next, we investigate whether the surface radiative energy balance allows us to identify candidate physical processes that explain these changes, and whether the processes identified using CESM1-CAM5 can be detected across the CMIP5 ensemble.

4 Observed and Simulated Surface Radiative Fluxes

4.1 CESM1-CAM5 Controlled Simulations

20   In Section 1 we discussed the expected direct effects of FIRE on surface longwave (LW) and shortwave (SW) fluxes and how these might be related to SIE. We begin our analysis with the downward fluxes at the surface, LW↓ and SW↓ in CESM1-CAM5 compared with CERES-EBAF Surface observations during their overlap period of 2001—2005. Uncertainties are based on the standard deviation of non-overlapping four-year periods from the rest of their records as described in Section 2. The CESM1 minus CERES-

25   EBAF Surface flux differences over 60—90 °N oceans are displayed in Figure 4 for each calendar month. As expected, inclusion of FIRE results in increased LW↓ and decreased SW↓, resulting in better agreement

with the observation-based CERES data. Absorbed longwave dominates, but CESM1-SoN's lower SIE results in a lower albedo that more than offsets the reduced $SW_\downarrow$ such that absorbed SW is also higher when including FIRE. The downward longwave is 11 W m^{-2} higher on average when including FIRE, which will increase mean ice temperature and increase heat input, resulting in a thinner pack that is more

5   vulnerable to warming.

It is also possible that local radiative feedbacks could be different when including or excluding FIRE. This would manifest as a change in the SoN minus NoS flux differences in time and is tested in Figure 5, which includes $SW_\downarrow$ and $LW_\downarrow$ differences for each season: December-January-February (DJF), March-April-May (MAM), June-July-August (JJA) and September-October-November (SON). Long-term

10   changes are estimated by multiplying the trend gradient by the length of the period, and the only significant ($p < 0.05$) changes occur in SON, where there is a decrease in the radiative flux difference between the two simulations.

However, the SoN minus NoS $LW_\downarrow$ trend is insignificantly positive during the first 70 years ($+0.08\pm0.09$ W m^{-2} yr^{-1}), so this change is not responsible for driving the faster disappearance of sea ice in CESM1-

15   SoN which has largely occurred by year 70. Instead, the difference appears related to differences in the relative effects of FIRE between icy and ice-free states. During the first 40 years when the simulations both have a healthy Arctic ice cover the median SON difference in $LW_\downarrow$ is 11.2 W m^{-2} (6.4—16.9 W m^{-2}, henceforth bracketed values are 14—86 % range) whereas for the final 40 years where both simulations are ice free during September, the difference is 6.8 (4.9—10.2) W m^{-2}. Some combination of cloud

20   properties or precipitation phase, such as the transition from snow to rain under warming, likely explain this difference.

Taken together, the energy budget analysis of CESM1-CAM5 1pctCO2 simulations indicates that differences in flux trends due to FIRE do not drive the faster observed retreat, but instead the effect of stronger year-round $LW_\downarrow$ in the initial state is the most important radiative contribution. This supports our

25   argument that the effective greenhouse effect from snowflakes results in a thinner pack whose retreat is more easily triggered by warming. This snowflake greenhouse effect is present year round and throughout the entire Arctic basin, leaving no safe spaces where the ice can fully recover.

4.2 CMIP5 Ensemble Results

The CESM1-CAM5 results show that snow radiative effects can substantially change simulated Arctic sea ice retreat under warming, which is consistent with the generally earlier disappearance of sea ice seen under historical-RCP8.5 simulations for the CMIP5-SoN sub-ensemble, compared with the CMIP5-NoS

5   ensemble. To investigate this, we consider the CMIP5 1979—2005 mean annual cycle and the 2006—2035 linear regression trends for each calendar month for a variety of properties in Figure 6. Each simulation's line is coloured according to whether it includes FIRE (SoN, blue) or excludes FIRE (NoS, red).

The mean state period is the overlap between NSIDC passive microwave sea ice extent data and the

10   historical simulations, and the trend period covers 30 years in which Figure 1 shows an apparent notable divergence in SIE between the CMIP5-SoN and CMIP5-NoS sub-ensembles.

Inspection of Figure 6 shows no clear support across the CMIP5 ensemble for the hypothesis we developed using the controlled CESM1-CAM5 simulations. In fact, two models that include FIRE show substantially more summertime $SW_\downarrow$, which is the opposite of the direct effects we hypothesise are related

15   to FIRE. These are the models GISS-E2-H and GISS-E2-R, whose CMIP5 versions greatly underestimated mean Ice Water Path (IWP) poleward of 60—90 °N (Stanfield et al., 2014). This illustrates how other differences aside from FIRE may well have compensating effects, showing that FIRE alone is insufficient to explain differences in Arctic sea ice retreat among models.

5 Discussion and Conclusions

20   The apparent agreement in September sea ice retreat between CMIP5-SoN and CESM1-SoN seen in Figure 1 and Figure 2 appears supportive of a major role for falling ice radiative effects in reinforcing Arctic sea ice retreat. However, analysis of the surface energy budget terms allowed us to identify a plausible physical mechanism in CESM1-CAM5, but revealed that the CMIP5 result was fortuitous and largely due to extremely early ice disappearance in the GISS-E2 models which accounted for two out of

25   seven of the sub-ensemble members. These models have been shown to drastically underestimate total

ice water path, resulting in too much surface shortwave radiation during summer and therefore likely a very strong surface albedo feedback.

The CMIP5 cross comparison simply shows that Arctic sea ice projections are at least as sensitive to other factors as to the inclusion or exclusion of FIRE. One example is the prevalence of mixed phase clouds with temperature: measurements with the lidar on the Cloud-Aerosol Lidar and Infrared Pathfinder Satellite Observations (CALIPSO) satellite show that supercooled liquid occurs at much lower temperatures than simulated in many models (Cesana et al., 2012, 2015). Most CMIP5 models display a strong negative shortwave cloud feedback at mid-to-high latitudes, some of which is related to melting of ice clouds into mixed-phase clouds, which are more effective reflectors of sunlight. The strength of this cooling feedback depends on the initial state, because one in which liquid clouds are already common means there will be less melting in future and therefore a weaker feedback. Controlled CESM1-CAM5 simulations shows differences in equilibrium climate sensitivity of greater than 1 °C per doubling of CO_2 when changing parameters that control these clouds (Tan et al., 2016). Such a large increase in warming would be expected to also change projected sea ice extent.

Furthermore, we did not explore any dynamic changes in response to the inclusion of FIRE. The magnitude of the radiative effects are a credible candidate for explaining major differences in sea ice extent, with 11 W m^{-2} of longwave over a year being sufficient to melt ~1 metre of ice over a year following a simple energy budget equation and assuming that all of the heat goes into the ice (Kay et al., 2008). For a mean state case this thinning is nonsensical since the ice warms and leaks some of this heat through increased longwave radiation, but it is consistent with our hypothesis of a substantial role for FIRE in Arctic melt. Nevertheless, changes in dynamics that affect patterns of cloudiness, ice transport or ocean heat transport could reinforce or counteract our proposed changes and we have not investigated these.

In conclusion, we do not argue that the exclusion of FIRE in current models necessarily means that Arctic sea ice will retreat faster than simulated by the average CMIP5 model. Inclusion of these effects followed by tuning may lead to counteracting processes. Or a model may have a stronger summertime albedo feedback than longwave-driven thinning effect, and show slower retreat once FIRE are included. However, our controlled experiments show a strong sensitivity of sea ice projections to FIRE in at least

one model, with Arctic sea ice retreat being approximately twice as fast once atmospheric CO_2 concentrations are above 2017 levels. Given that the snow radiative effect exists in reality, we encourage other modelling groups to include them in future cloud schemes to increase confidence in Arctic sea ice projections.

Data availability. The NSIDC [ftp://sidads.colorado.edu/DATASETS/NOAA/G02135/north/monthly/data/], CERES-EBAF [https://ceres.larc.nasa.gov/order_data.php] and CMIP5 data [https://cmip.llnl.gov/cmip5/data_portal.html] are available from public archives. The time series of CMIP5 and CESM1 sea ice and radiative fluxes are appended as supplementary information.

Author contributions. JLL led the research and performed CMIP5 output & CESM1 sensitivity output processing & analysis. WLL conducted CESM1 model sensitivity runs. MR performed the CMIP5 processing & analysis and the time series analysis. YHW & YLH & JYY provided discussion & editing. EF & JJ & GS supported and offered comments/suggestions to the study. YL quality controlled the data.

Competing interests. The authors declare no competing interests.

Acknowledgements. MR thanks Dr. Kirchmeier-Young for providing her CMIP5 sea ice extent series to allow verification of his code.

References

Bintanja, R. and Selten, F. M.: Future increases in Arctic precipitation linked to local evaporation and sea-ice retreat, Nature, 509(7501), 479–482, doi:10.1038/nature13259, 2014.

Boisvert, L. N. and Stroeve, J. C.: The Arctic is becoming warmer and wetter as revealed by the Atmospheric Infrared Sounder, Geophys. Res. Lett., 42(11), 4439–4446, doi:10.1002/2015GL063775,

2015.

Cavalieri, D. J., Crawford, J. P., Drinkwater, M. R., Eppler, D. T., Farmer, L. D., Jentz, R. R. and Wackerman, C. C.: Aircraft active and passive microwave validation of sea ice concentration from the Defense Meteorological Satellite Program special sensor microwave imager, J. Geophys. Res., 96(C12),

5   21989, doi:10.1029/91JC02335, 1991.

Cesana, G., Kay, J. E., Chepfer, H., English, J. M. and de Boer, G.: Ubiquitous low-level liquid-containing Arctic clouds: New observations and climate model constraints from CALIPSO-GOCCP, Geophys. Res. Lett., 39(20), n/a-n/a, doi:10.1029/2012GL053385, 2012.

Cesana, G., Waliser, D. E., Jiang, X. and Li, J.-L. F.: Multimodel evaluation of cloud phase transition

10   using   satellite   and   reanalysis   data,   J.   Geophys.   Res.   Atmos.,   120(15),   7871–7892, doi:10.1002/2014JD022932, 2015.

Cohen, J., Screen, J. A., Furtado, J. C., Barlow, M., Whittleston, D., Coumou, D., Francis, J., Dethloff, K., Entekhabi, D., Overland, J. and Jones, J.: Recent Arctic amplification and extreme mid-latitude weather, Nat. Geosci., 7(9), 627–637, doi:10.1038/ngeo2234, 2014.

15   Fetterer, F., Knowles, K., Meier, W., Savoie, M. and Windnagel, A. K.: updated daily. Sea Ice Index, Version 3 [NH Monthly Sea Ice Extent], Boulder, Color. USA. NSIDC Natl. Snow Ice Data Cent., doi:10.7265/N5K072F8, 2017.

Forster, P. M., Andrews, T., Good, P., Gregory, J. M., Jackson, L. S. and Zelinka, M.: Evaluating adjusted forcing and model spread for historical and future scenarios in the CMIP5 generation of climate models,

20   J. Geophys. Res. Atmos., 118(3), 1139–1150, doi:10.1002/jgrd.50174, 2013.

Francis, J. A. and Vavrus, S. J.: Evidence linking Arctic amplification to extreme weather in mid-latitudes, Geophys. Res. Lett., 39(6), n/a-n/a, doi:10.1029/2012GL051000, 2012.

Gettelman, A., Liu, X., Ghan, S. J., Morrison, H., Park, S., Conley, A. J., Klein, S. A., Boyle, J., Mitchell, D. L. and Li, J.-L. F.: Global simulations of ice nucleation and ice supersaturation with an improved cloud

25   scheme   in   the   Community   Atmosphere   Model,   J.   Geophys.   Res.,   115(D18),   D18216, doi:10.1029/2009JD013797, 2010.

Hansen, J., Sato, M. and Ruedy, R.: Radiative forcing and climate response, J. Geophys. Res. Atmos., 102(D6), 6831–6864, doi:10.1029/96JD03436, 1997.

Jacob, T., Wahr, J., Pfeffer, W. T. and Swenson, S.: Recent contributions of glaciers and ice caps to sea level rise, Nature, 482(7386), 514–518, doi:10.1038/nature10847, 2012.

Kato, S., Loeb, N. G., Rutan, D. A., Rose, F. G., Sun-Mack, S., Miller, W. F. and Chen, Y.: Uncertainty Estimate of Surface Irradiances Computed with MODIS-, CALIPSO-, and CloudSat-Derived Cloud and Aerosol Properties, Surv. Geophys., 33(3–4), 395–412, doi:10.1007/s10712-012-9179-x, 2012.

Kato, S., Loeb, N. G., Rose, F. G., Doelling, D. R., Rutan, D. A., Caldwell, T. E., Yu, L. and Weller, R. A.: Surface Irradiances Consistent with CERES-Derived Top-of-Atmosphere Shortwave and Longwave Irradiances, J. Clim., 26(9), 2719–2740, doi:10.1175/JCLI-D-12-00436.1, 2013.

Kay, J. E., L'Ecuyer, T., Gettelman, A., Stephens, G. and O'Dell, C.: The contribution of cloud and radiation anomalies to the 2007 Arctic sea ice extent minimum, Geophys. Res. Lett., 35(8), L08503, doi:10.1029/2008GL033451, 2008.

Kay, J. E., Holland, M. M. and Jahn, A.: Inter-annual to multi-decadal Arctic sea ice extent trends in a warming world, Geophys. Res. Lett., 38(15), n/a-n/a, doi:10.1029/2011GL048008, 2011.

Kirchmeier-Young, M. C., Zwiers, F. W. and Gillett, N. P.: Attribution of Extreme Events in Arctic Sea Ice Extent, J. Clim., 30(2), 553–571, doi:10.1175/JCLI-D-16-0412.1, 2017.

Kjeldsen, K. K., Korsgaard, N. J., Bjørk, A. A., Khan, S. A., Box, J. E., Funder, S., Larsen, N. K., Bamber, J. L., Colgan, W., van den Broeke, M., Siggaard-Andersen, M.-L., Nuth, C., Schomacker, A., Andresen, C. S., Willerslev, E. and Kjær, K. H.: Spatial and temporal distribution of mass loss from the Greenland Ice Sheet since AD 1900, Nature, 528(7582), 396–400, doi:10.1038/nature16183, 2015.

Kurtz, N. T. and Markus, T.: Satellite observations of Antarctic sea ice thickness and volume, J. Geophys. Res. Ocean., 117(C8), n/a-n/a, doi:10.1029/2012JC008141, 2012.

Kwok, R. and Cunningham, G. F.: ICESat over Arctic sea ice: Estimation of snow depth and ice thickness, J. Geophys. Res., 113(C8), C08010, doi:10.1029/2008JC004753, 2008.

Li, J.-L. F., Lee, W.-L., Waliser, D. E., David Neelin, J., Stachnik, J. P. and Lee, T.: Cloud-precipitation-radiation-dynamics interaction in global climate models: A snow and radiation interaction sensitivity experiment, J. Geophys. Res. Atmos., 119(7), 3809–3824, doi:10.1002/2013JD021038, 2014.

Li, J.-L. F., Richardson, M., Hong, Y., Lee, W.-L., Wang, Y.-H., Yu, J.-Y., Fetzer, E., Stephens, G. and Liu, Y.: Improved simulation of Antarctic sea ice due to the radiative effects of falling snow, Environ.

Res. Lett., 12(8), doi:10.1088/1748-9326/aa7a17, 2017.

Massonnet, F., Fichefet, T., Goosse, H., Bitz, C. M., Philippon-Berthier, G., Holland, M. M. and Barriat, P.-Y.: Constraining projections of summer Arctic sea ice, Cryosph., 6(6), 1383–1394, doi:10.5194/tc-6-1383-2012, 2012.

Morrison, H. and Gettelman, A.: A New Two-Moment Bulk Stratiform Cloud Microphysics Scheme in the Community Atmosphere Model, Version 3 (CAM3). Part I: Description and Numerical Tests, J. Clim., 21(15), 3642–3659, doi:10.1175/2008JCLI2105.1, 2008.

Overeem, I., Anderson, R. S., Wobus, C. W., Clow, G. D., Urban, F. E. and Matell, N.: Sea ice loss enhances wave action at the Arctic coast, Geophys. Res. Lett., 38(17), n/a-n/a, doi:10.1029/2011GL048681, 2011.

Post, E., Steinman, B. A. and Mann, M. E.: Acceleration of phenological advance and warming with latitude over the past century, Sci. Rep., 8(1), 3927, doi:10.1038/s41598-018-22258-0, 2018.

Riahi, K., Rao, S., Krey, V., Cho, C., Chirkov, V., Fischer, G., Kindermann, G., Nakicenovic, N. and Rafaj, P.: RCP 8.5—A scenario of comparatively high greenhouse gas emissions, Clim. Change, 109(1–2), 33–57, doi:10.1007/s10584-011-0149-y, 2011.

Rolph, R. J., Mahoney, A. R., Walsh, J. and Loring, P. A.: Impacts of a lengthening open water season on Alaskan coastal communities: deriving locally relevant indices from large-scale datasets and community observations, Cryosph., 12(5), 1779–1790, doi:10.5194/tc-12-1779-2018, 2018.

Shiklomanov, N. I., Streletskiy, D. A., Swales, T. B. and Kokorev, V. A.: Climate Change and Stability of Urban Infrastructure in Russian Permafrost Regions: Prognostic Assessment based on GCM Climate Projections, Geogr. Rev., 107(1), 125–142, doi:10.1111/gere.12214, 2017.

Smedsrud, L. H., Halvorsen, M. H., Stroeve, J. C., Zhang, R. and Kloster, K.: Fram Strait sea ice export variability and September Arctic sea ice extent over the last 80 years, Cryosph., 11(1), 65–79, doi:10.5194/tc-11-65-2017, 2017.

Smith, L. C. and Stephenson, S. R.: New Trans-Arctic shipping routes navigable by midcentury, Proc. Natl. Acad. Sci., 110(13), E1191–E1195, doi:10.1073/pnas.1214212110, 2013.

Stanfield, R. E., Dong, X., Xi, B., Kennedy, A., Del Genio, A. D., Minnis, P. and Jiang, J. H.: Assessment of NASA GISS CMIP5 and Post-CMIP5 Simulated Clouds and TOA Radiation Budgets Using Satellite

Observations. Part I: Cloud Fraction and Properties, J. Clim., 27(11), 4189–4208, doi:10.1175/JCLI-D-13-00558.1, 2014.

Stroeve, J. C., Kattsov, V., Barrett, A., Serreze, M., Pavlova, T., Holland, M. and Meier, W. N.: Trends in Arctic sea ice extent from CMIP5, CMIP3 and observations, Geophys. Res. Lett., 39(16), n/a-n/a,

5 doi:10.1029/2012GL052676, 2012.

Tan, I., Storelvmo, T. and Zelinka, M. D.: Observational constraints on mixed-phase clouds imply higher climate sensitivity, Science (80-.)., 352(6282), 224–227, doi:10.1126/science.aad5300, 2016.

Taylor, K. E., Stouffer, R. J. and Meehl, G. A.: An Overview of CMIP5 and the Experiment Design, Bull. Am. Meteorol. Soc., 93(4), 485–498, doi:10.1175/BAMS-D-11-00094.1, 2012.

10 Tietsche, S., Notz, D., Jungclaus, J. H. and Marotzke, J.: Recovery mechanisms of Arctic summer sea ice, Geophys. Res. Lett., 38(2), n/a-n/a, doi:10.1029/2010GL045698, 2011.

Zhang, J., Lindsay, R., Steele, M. and Schweiger, A.: What drove the dramatic retreat of arctic sea ice during summer 2007?, Geophys. Res. Lett., 35(11), L11505, doi:10.1029/2008GL034005, 2008.
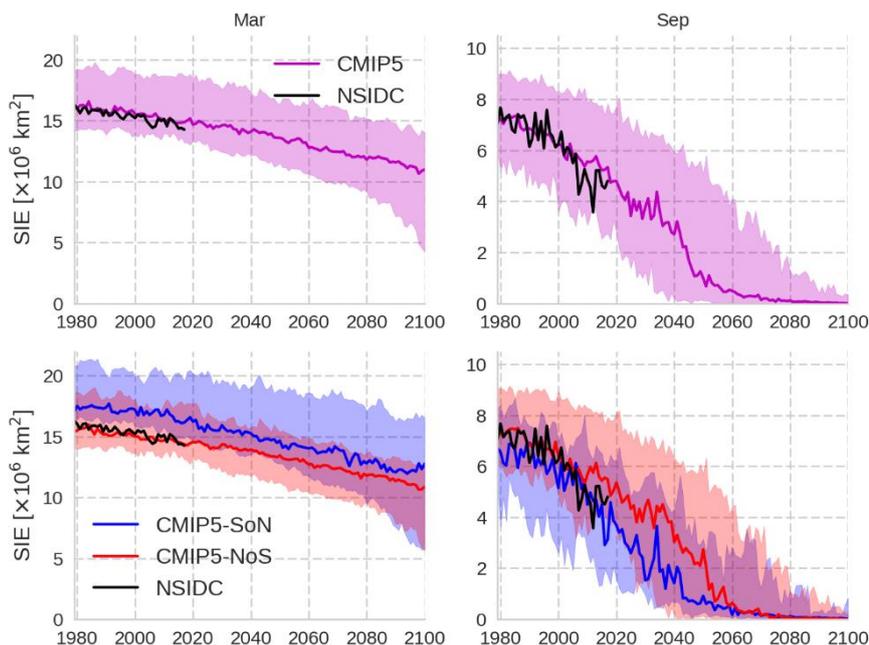
Figure 1: Arctic sea ice extent during March (left) and September (right) in NSIDC observations (black) and CMIP5 climate models (line median, shaded 10—90 % range). The upper row shows the full CMIP5 ensemble. The bottom row shows the ensemble split into those including snow radiative effects (blue) and those excluding snow radiative effects (red).
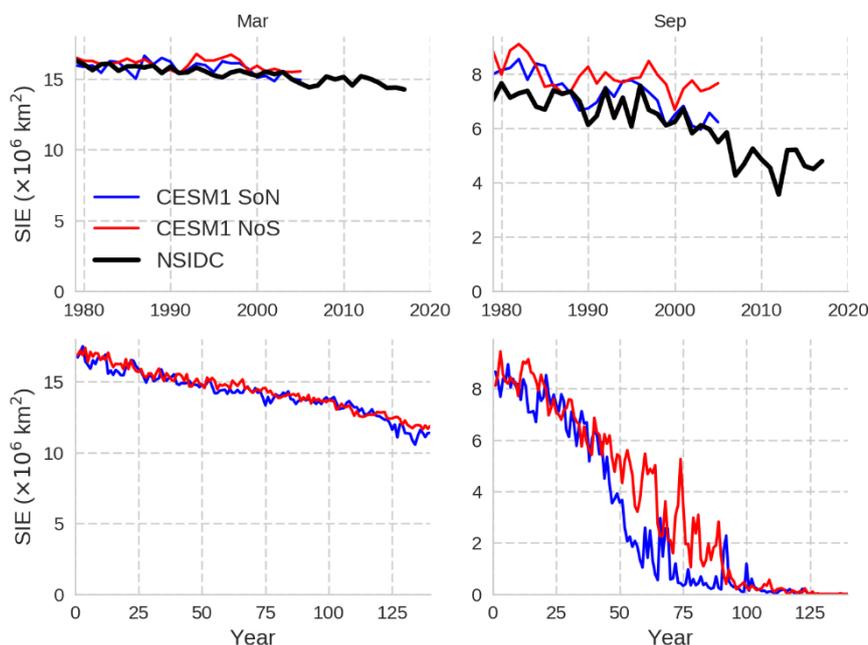
Figure 2: Observed (black) CESM1-CAM5 simulated Arctic sea ice extent in March (left) and September (right). Blue lines are with snow radiative effects (SoN) and red without (NoS). The upper panels are historical, the lower panels from 1pctCO2.
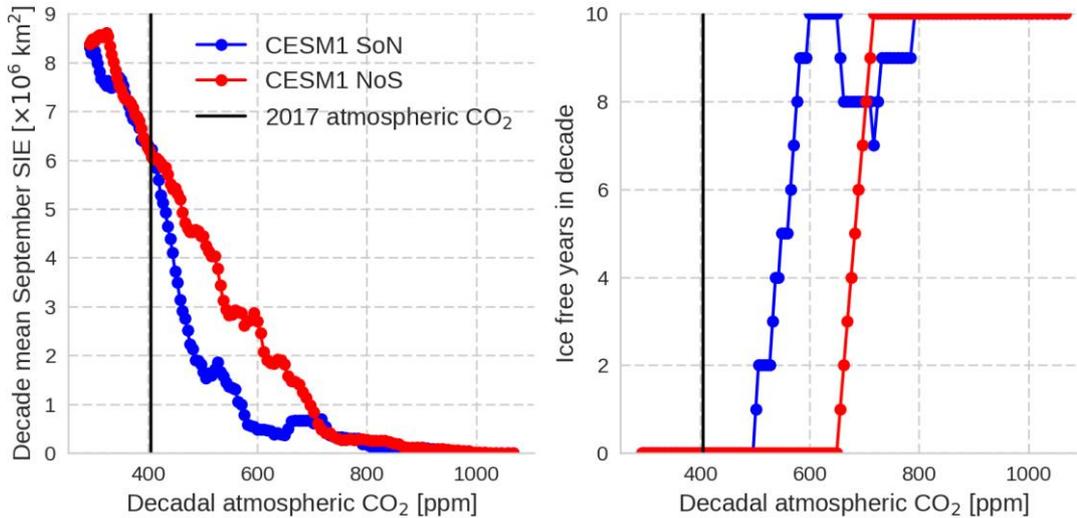
Figure 3: Changes in September Arctic sea ice under 1 % yr⁻¹ CO_2 increases for CESM1 SoN (blue) and CESM1 NoS (red) as a function of decade-mean atmospheric CO_2. Left shows the decadal mean sea ice extent and right shows the number of years within that decade for which SIE < 1×10⁶ km², commonly taken as representative of an ice-free Arctic Ocean basin. The atmospheric CO_2 concentration in 2017 is shown as a vertical black line in each case, but any comparisons must be carefully made since the real world includes changes in non-CO_2 forcing.
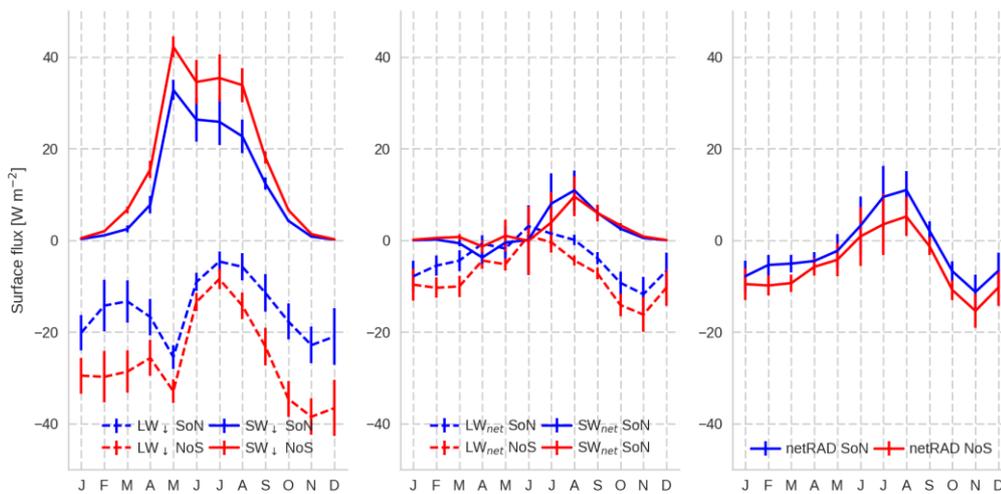
Figure 4: CESM1 minus CERES 60—90 °N ocean differences in mean surface fluxes for each calendar month over 2001—2005. The difference using CESM1-SoN (blue) and CESM1-NoS (red) are both shown, and error bars are estimates of uncertainty due to internal variability from selecting the four year overlap period, based on the spread compared with other four-year periods in both CERES (post-2005) and CESM1 (pre-2001). Left panel: differences in downward longwave

(dashed) and downward shortwave (solid). Centre panel: difference in net longwave (dashed, positive downward) and net shortwave (solid). Right panel: net downward radiation sum.
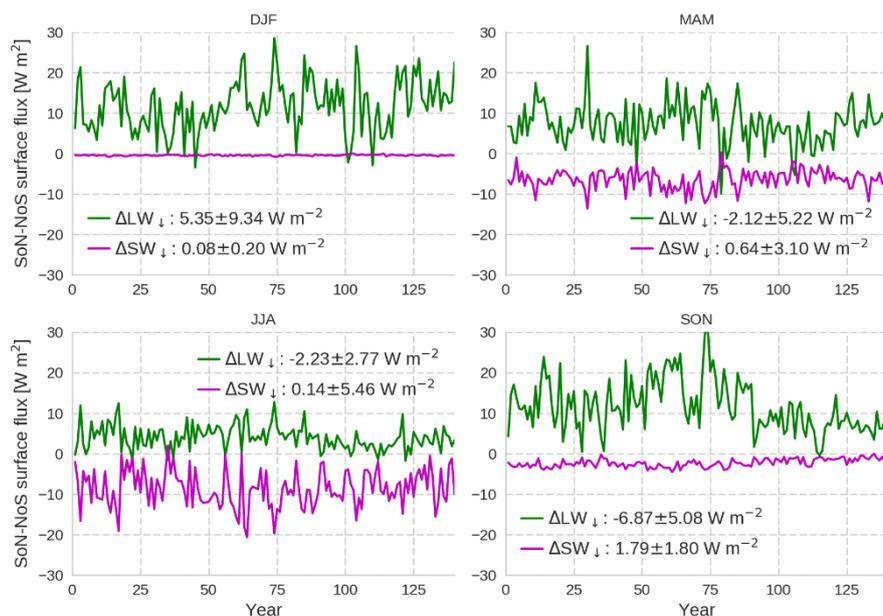
Figure 5: CESM1-SoN minus CESM1-NoS season differences in downward surface fluxes over 60—90 °N oceans. The legend reports the estimate of the 140-year change in this difference by multiplying the linear regression trend coefficient by 140, with ±2σ uncertainties.
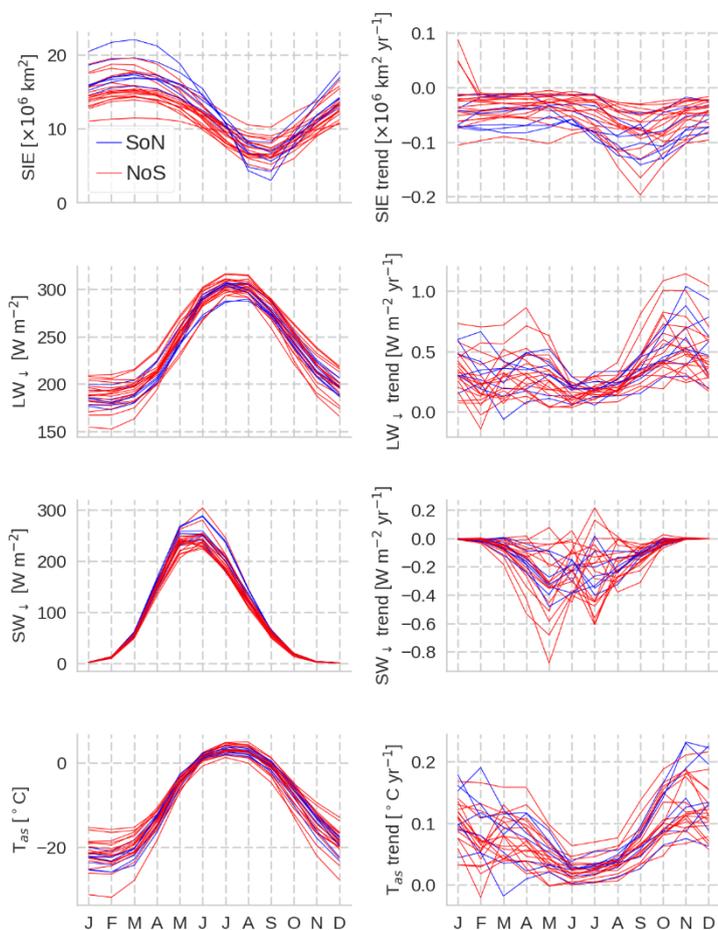
Figure 6: Output over 60—90 °N oceans from individual CMIP5 historical-RCP8.5 simulations according to whether the simulation includes FIRE (blue) or excludes them (red). Left panels show annual cycles of mean properties from 1979—2005 and right panels show the trend for each calendar month over 2006—2035. From top to bottom the properties are: sea ice extent (poleward of 30°), downward longwave at the surface, downward shortwave at the surface and near-surface air temperature.